Efficient Design of Cosine-Modulated Filter Banks via Convex Optimization

Ha Hoang Kha, Hoang Duong Tuan, and Truong Q. Nguyen

***Abstract*—This paper presents efficient approaches for designing cosine-modulated filter banks with linear phase prototype filter. First, we show that the design problem of the prototype filter being a spectral factor of $2M$th-band filter is a nonconvex optimization problem with low degree of nonconvexity. As a result, the nonconvex optimization problem can be cast into a semi-definite programming (SDP) problem by a convex relaxation technique. Then the reconstruction error is further minimized by an efficient iterative algorithm in which the closed-form expression is given in each iteration. Several examples are given to illustrate the effectiveness of the proposed method over the existing ones.**

***Index Terms*—Convex optimization, cosine-modulated filter bank, prototype filter, semidefinite programming.**

I. Introduction

COSINE-MODULATED finite-impulse-response (FIR) filter banks are used extensively in applications that include data compression (speech, audio, image, and video), denoising, feature detection and extraction [1], [5], [14], [19]. They are a special subclass of the general M-channel filter banks shown in Fig. 1, where analysis filters $H_k(z)$ and synthesis filters $F_k(z)$ can be obtained by modulating the coefficient values of a prototype filter. As a result, the design of the cosine-modulated filter bank (CMFB) reduces to that of the prototype filter. Moreover, there are efficient structures with a fast transform for modulation, so the cost of the analysis bank is equal to that of one filter plus modulation overhead [14], [19].

The CMFB design problem has been extensively studied (see e.g., [12]–[14], [19] and references therein). For pseudo-QMF banks, the analysis and synthesis filters must be carefully chosen so that significant aliasing terms are cancelled, and the distortion function $T_0(e^{j\omega})$ is linear phase. At the end, the CMFB design problem is reduced to finding a linear phase prototype filter with high stopband attenuation that provides a flat overall magnitude response $|T_0(e^{j\omega})|$. As analyzed in details in [12], the design effectiveness is gauged by the stopband attenuation performance because the latter poses the most challenge. Another criterion that is often ignored in most designs [2], [10], [12], [13], [19] is narrow transition bandwidth. There are two approaches to address the prototype filter design and both of them are based on optimization. The first approach aims at designing a good linear phase lowpass filter (by Parks–McClellan algorithm [2] or the Kaiser window method [10]) and then tunes the transition bandwidth (the only free parameter in these designs) to meet the $2M$th band condition approximately. As the transition bandwidth is not controlled, the small reconstruction error is not easily achieved although the high stopband attenuation is attained. The still good performance of these designs indicates that the $2M$th band condition might not be really hard in the class of lowpass linear phase filters. A design method of lowpass filters approximately being a spectral factor of a $2M$th band filter has been also developed in [8], where the transition bandwidth can be effectively controlled. In contrast, the second approach aims at meeting the perfect $2M$th band condition first and then the stopband attenuation is optimized [12], [13], [19]. The lattice factorization based formulation [19] leads to a highly nonlinear and nonconvex optimization problem that is not easily computed. Therefore, it is difficult to obtain a filter bank with high stopband attenuation. Much more direct formulations given in [5], [12], and [13] lead to the minimization of a convex quadratic objective function over nonconvex quadratic constraints by the $2M$th band condition. The nonconvex quadratic optimization is still a very difficult class of optimization and there is no practical algorithm for locating its global optimal solution [18]. However, still very good solutions have been found in [12] and [13] by local optimization algorithms in reasonable computational time. This again indicates that the $2M$th band condition might appear not so challenging and there is a hidden partial convex structure in its quadratic constraint formulation. Recently, there are many iterative methods developed for solving the cosine-modulated filter bank design problem. In [3], [20], quadratic constraints are linearized, whereas in [11], the perfect reconstruction condition, which is expressed as an fourth-order objective function, is linearized. In [6], the iterative modified Newton method is applied

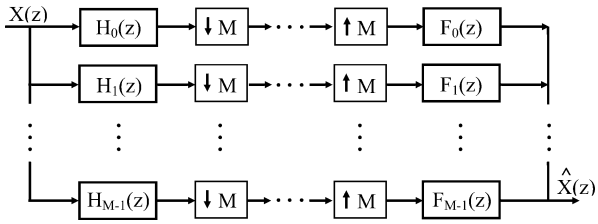

Fig. 1. M-channel maximally decimated filter bank.

Manuscript received February 05, 2007; revised June 15, 2008. First published November 11, 2008; current version published February 13, 2009. The associate editor coordinating the review of this manuscript and approving it for publication was Dr. Gerald Schuller.

H. H. Kha and H. D. Tuan are with the School of Electrical Engineering and Telecommunications, University of New South Wales, UNSW Sydney, NSW 2052, Australia (e-mail: h.kha@student.unsw.edu.au; h.d.tuan@unsw.edu.au).

T. Q. Nguyen is with the Department of Electrical and Computer Engineering, University of California in San Diego, La Jolla, CA 92093-0407 USA (e-mail: nguyent@ece.ucsd.edu).

Digital Object Identifier 10.1109/TSP.2008.2009268

to find lattice coefficients and prototype filter coefficients such that the stopband energy of the prototype filter is minimized.

In this paper, we explore partial convex structures of the optimization formulation for effective computation and design. In contrast with [2] and [10]–[13], we formulate the CMFB design based on the product filter. The problem is then recast as SDP that can be effectively computed. The conventional spectral factorization to recover a filter from its product is computationally expensive and numerically unstable, especially for filters with high stopband attenuation [19]. Moreover, it is not guaranteed to obtain the linear phase spectral factor. However, due to our formulation, the optimal linear phase prototype filter can be easily obtained by singular value decomposition of a positive semi-definite matrix. Additionally, to improve the reconstruction error for filters with high order, we propose an efficient iterative algorithm, in which the closed-form expression is obtained in iterations. We also provide numerical examples to verify the viability of our approach.

This paper is organized as follows. In Section II, we review the derivation of quadratically constrained quadratic optimization formulation of CMFB designs. In Section III, the degree of nonconvexity of the optimization problem is analyzed, and then the SDP relaxation technique is introduced. The improvement solution by a cheap iterative algorithm is described in Section IV. Several example designs are given in Section V. Finally, concluding remarks are made in Section VI.

Notations: Bold-faced characters denote matrices and column vectors, with upper case used for the former and lower case for the latter. The notation $\mathbf{X} \geq 0$ denotes a (symmetric) positive semi-definite matrix. The inner product $\langle \mathbf{X}, \mathbf{Y} \rangle$ between the matrices $\mathbf{X}$ and $\mathbf{Y}$ is defined as $\mathrm{Trace}\,(\mathbf{XY})$, i.e., $\langle \mathbf{X}, \mathbf{Y} \rangle = \mathrm{Trace}(\mathbf{XY})$. The inner product between vectors $\mathbf{x}$ and $\mathbf{y}$ is defined as $\langle \mathbf{x}, \mathbf{y} \rangle = \mathbf{x}^T\mathbf{y}$. For a given set $\mathcal{C} \in \mathbb{R}^L$ its convex hull (conic hull), denoted by $\mathrm{conv}(\mathcal{C})(\mathrm{cone}(\mathcal{C}))$, is the smallest convex set (cone) in $\mathbb{R}^L$ that contains $\mathcal{C}$. The polar set of $\mathcal{C}$ is the cone $\mathcal{C}^* = \{\mathbf{x} : \langle \mathbf{x}, \mathbf{y} \rangle \geq 0, \forall \mathbf{y} \in \mathcal{C}\}$. Furthermore, the value of the function, $\lfloor x \rfloor$, is the largest integer less than or equal to x.

An earlier version of part of this work has been reported in a conference paper [7]. This paper presents a more complete version of the work.

II. Cosine-Modulated Filter Banks

In cosine-modulated QMF banks, all the analysis and synthesis filters can be generated by modulating a lowpass linear phase prototype filter. Let $H(z)$ denote the transfer function of the prototype filter as given by

$$H(z) = \sum_{n=0}^{N} h(n) z^{-n}, \text{with } h(n) = h(N-n). \tag{1}$$

Then the analysis and synthesis filters are given by

$$h_k(n) = 2h(n)\cos\left(\frac{\pi}{M}(k+0.5)\left(n-\frac{N}{2}\right)+\theta_k\right)$$
$$f_k(n) = 2h(n)\cos\left(\frac{\pi}{M}(k+0.5)\left(n-\frac{N}{2}\right)-\theta_k\right)$$

where $h_k(n)$ and $f_k(n)$, $0 \leq k \leq M-1$, $0 \leq n \leq N$ represent the impulse responses of the kth channel analysis and synthesis filters, respectively. In the M-channel maximally decimated filter bank shown in Fig. 1, the reconstructed signal $\hat{X}(z)$ can be written in terms of these filters in the z-domain as

$$\hat{X}(z) = X(z)T_0(z) + \sum_{l=1}^{M-1} X(ze^{-j2\pi l/M})T_l(z) \tag{2}$$

where

$$T_l(z) = \frac{1}{M}\sum_{k=0}^{M-1} H_k(ze^{-j2\pi l/M})F_k(z).$$

Here, $T_0(z)$ is the overall distortion transfer function and $T_l(z), l \neq 0$ is the aliasing transfer function. To cancel aliasing and achieve perfect reconstruction, it is required that

$$\begin{aligned} &T_l(z) = 0, \text{ for } l = 1, 2, \ldots, M-1 \\ &T_0(z) = cz^{-n_d}, c \neq 0, n_d \text{ is positive integer.} \end{aligned} \tag{3}$$

As the analysis and synthesis filters have narrow transition bands and high stopband attenuation, the overlap between nonadjacent filters is negligible. Moreover, it was shown in [12] that significant aliasing terms from the overlap of the adjacent filters are cancelled by choosing $\theta_k = (-1)^k\pi/4$. Under these circumstances, the overall distortion function is given by

$$T_0(e^{j\omega}) = \frac{e^{-j\omega N}}{M}\sum_{k=0}^{2M-1} |H(e^{j(\omega-k\pi/M-\pi/2M)})|^2. \tag{4}$$

To eliminate amplitude distortion, $|T_0(e^{j\omega})|$ must be constant for all frequencies. It is equivalent to

$$\sum_{k=0}^{2M-1} |H(e^{j(\omega-k\pi/M)})|^2 = 1 \quad \forall \omega \in [0, \pi]. \tag{5}$$

The above condition means that the magnitude squared response $|H(e^{j\omega})|^2$ is a $2M$th band filter [14], [19]. Therefore, by introducing the product filter $G(z) = H(z)H(z^{-1})$, $G(z)$ is then a zero phase filter with the frequency response

$$G(\omega) = \sum_{i=0}^{N} g_i \cos(i\omega) = |H(e^{j\omega})|^2. \tag{6}$$

For the sake of simplicity, we will focus on the prototype filter order is even, i.e., $N = 2L$, then the frequency response $H(e^{j\omega})$ is of the form $H(e^{j\omega}) = e^{-j\omega L}H_R(\omega)$, where $H_R(\omega)$ is the amplitude response of $H(e^{j\omega})$. Here, $H_R(\omega)$ is given by

$$H_R(\omega) = \sum_{n=0}^{L} b_n \cos\omega n = \langle \mathbf{b}, \boldsymbol{\varphi}_L(\omega) \rangle \tag{7}$$

where

$$\begin{aligned} \mathbf{b} &= [b_0 \ b_1 \cdots b_L]^T = [h_L \ 2h_{L-1} \cdots 2h_0]^T \\ \boldsymbol{\varphi}_L(\omega) &= [1 \ \cos\omega \cdots \cos L\omega]^T. \end{aligned}$$

Then, (6) can be rewritten in vector form

$$G(\omega) = \langle \mathbf{g}, \boldsymbol{\varphi}_N(\omega) \rangle = \langle \mathbf{b}, \boldsymbol{\varphi}_L(\omega) \rangle^2 \tag{8}$$

where $\mathbf{g} = [g_0 \;\; g_1 \cdots g_{N-1} \;\; g_N]^T$. In the terms of the product filter coefficients, the constraint (5) can be written as

$$g_{2Mi} = \frac{1}{2M}\delta(i), \quad i = 0, 1, \ldots, \left\lfloor \frac{L}{M} \right\rfloor. \tag{9}$$

Let $\mathcal{C}$ denote the set of all possible product filters such that there exist linear phase spectral factors. In other words, $\mathbf{g} \in \mathcal{C}$ if and only if $\mathbf{g}$ satisfies (8) for some $\mathbf{b} \in \mathbb{R}^{L+1}$. The set $\mathcal{C}$ is mathematically expressed as

$$\mathcal{C} = \{\mathbf{g} \in \mathbb{R}^{N+1} : G(\omega) = \langle \mathbf{g}, \boldsymbol{\varphi}_N(\omega) \rangle = \langle \mathbf{b}, \boldsymbol{\varphi}_L(\omega) \rangle^2 \text{ for some } \mathbf{b} \in \mathbb{R}^{L+1}\}$$

or, equivalently

$$\mathcal{C} = \{\mathbf{g} \in \mathbb{R}^{N+1} : G(\omega) = \langle \mathbf{g}, \boldsymbol{\varphi}_N(\omega) \rangle = \langle \mathbf{b}\mathbf{b}^T, \boldsymbol{\mathcal{T}}_L(\omega) \rangle \text{ for some } \mathbf{b} \in \mathbb{R}^{L+1}\} \tag{10}$$

where the Lth-order trigonometric moment matrix $\boldsymbol{\mathcal{T}}_L(\omega)$ is defined as the $(L+1) \times (L+1)$ positive-semidefinite matrix [see (11), shown at the bottom of the page]. Alternatively, matrix $\boldsymbol{\mathcal{T}}_L(\omega)$ can be expressed as an affine combination of symmetric matrices

$$\boldsymbol{\mathcal{T}}_L(\omega) = \sum_{k=0}^{2L} \cos k\omega \boldsymbol{\mathcal{M}}_k \tag{12}$$

where the $(L+1) \times (L+1)$ symmetric matrix $\boldsymbol{\mathcal{M}}_k$ has (i,j)th element

$$\boldsymbol{\mathcal{M}}_k(i,j) = \frac{1}{2}(\delta(|i+j| - k) + \delta(|i-j| - k)), \quad 0 \le i \le L, \quad 0 \le j \le L.$$

Substituting $\boldsymbol{\mathcal{T}}_L(\omega)$ into (10) and equating the terms with the same $\cos k\omega$, we obtain the relationship between $\mathbf{g}$ and $\mathbf{b}$ in time domain

$$g_i = \langle \mathbf{b}\mathbf{b}^T, \boldsymbol{\mathcal{M}}_i \rangle. \tag{13}$$

Consequently, the $2M$th band condition (9) can be written as

$$g_{2Mi} = \langle \mathbf{b}\mathbf{b}^T, \boldsymbol{\mathcal{M}}_{2Mi} \rangle = \frac{1}{2M}\delta(i), \quad i = 0, 1, \ldots, \left\lfloor \frac{L}{M} \right\rfloor. \tag{14}$$

Hence, the CMFB design problem is to find the prototype filter $H(e^{j\omega})$ which has high stopband attenuation and satisfies the (14). The weighted stopband energy can be defined as

$$\xi = \frac{1}{\pi}\sum_{i=1}^{K} W_i \int_{\omega_{i-1}}^{\omega_i} |H(e^{j\omega})|^2 d\omega \tag{15}$$

where K is the number of frequency bands in the stopband, and ω_i are the band edges of the stopband with $\omega_0 = \omega_s$ and $\omega_K = \pi$. The relative weights $W_i > 0$ can be chosen to emphasize the certain regions of the stopband energy spectrum. We can rewrite

$$\begin{aligned}\xi &= \frac{1}{\pi}\sum_{i=1}^{K} W_i \int_{\omega_{i-1}}^{\omega_i} \mathbf{b}^T \boldsymbol{\varphi}_L(\omega)\boldsymbol{\varphi}_L^T(\omega)\mathbf{b} d\omega \\ &= \mathbf{b}^T \mathbf{Q} \mathbf{b} = \langle \mathbf{b}\mathbf{b}^T, \mathbf{Q} \rangle\end{aligned}$$

where $\mathbf{Q}$ is a real, symmetric, positive-definite matrix given by

$$\mathbf{Q} = \frac{1}{\pi}\sum_{i=1}^{K} W_i \int_{\omega_{i-1}}^{\omega_i} \boldsymbol{\varphi}_L(\omega)\boldsymbol{\varphi}_L^T(\omega) d\omega.$$

Finally, in terms of the prototype filter, the filter bank design problem can be expressed as

$$\min_{\mathbf{b}} \quad \langle \mathbf{b}\mathbf{b}^T, \mathbf{Q} \rangle \tag{17a}$$

$$\text{subject to:} \quad \langle \mathbf{b}\mathbf{b}^T, \boldsymbol{\mathcal{M}}_{2Mi} \rangle = \frac{1}{2M}\delta(i), \quad i = 0, 1, \ldots, \left\lfloor \frac{L}{M} \right\rfloor. \tag{17b}$$

The above optimization problem minimizes a quadratic objective function subject to quadratic equality constraints. Note that $\mathbf{Q}$ is a positive definite matrix, so the objective function is convex. However, the matrices $\boldsymbol{\mathcal{M}}_{2Mi}$ are symmetric, but indefinite. Therefore, the problem (17) is a nonconvex quadratically constrained optimization problem. It is very hard to find the globally optimal solution due to the existence of local minima [17], [18].

Alternatively, in the terms of the product filter, the filter bank design problem (17) can be given by

$$\min_{\mathbf{g}} \quad \langle \mathbf{c}, \mathbf{g} \rangle \tag{18a}$$

$$\text{subject to:} \quad g_{2Mi} = \frac{1}{2M}\delta(i), \quad i = 0, 1, \ldots, \left\lfloor \tfrac{L}{M} \right\rfloor, \tag{18b}$$

$$\mathbf{g} \in \mathcal{C} \tag{18c}$$

where $\mathbf{c} = (1)(\pi)\sum_{i=1}^{K} W_i \int_{\omega_{i-1}}^{\omega_i} \boldsymbol{\varphi}_N(\omega) d\omega$. It should be noted that the product filter based methods [9], [14], [19] only require

$$\boldsymbol{\mathcal{T}}_L(\omega) = \boldsymbol{\varphi}_L(\omega)\boldsymbol{\varphi}_L^T(\omega) = \begin{bmatrix} 1 & \cos\omega & \cdots & \cos L\omega \\ \cos\omega & \frac{\cos 2\omega + 1}{2} & \cdots & \frac{\cos(L+1)\omega + \cos(L-1)\omega}{2} \\ \cdots & \cdots & \cdots & \cdots \\ \cos L\omega & \frac{\cos(L+1)\omega + \cos(L-1)\omega}{2} & \cdots & \frac{\cos 2L\omega + 1}{2} \end{bmatrix} \tag{11}$$

$G(e^{j\omega}) \geq 0 \forall \omega$ to guarantee the existence of the prototype filter, but not ensure the existence of the linear phase prototype filter. In our formulation (18), the more restrictive condition, $\mathbf{g} \in \mathcal{C}$, is imposed on the product filter to ensure that the linear phase prototype filter can be recovered from the optimal product filter.

In conventional spectral factorization based methods, the product filter $G(z)$ is designed to satisfy the $2M$th-band condition (14). Then, the linear phase prototype filter can be approximately found by the iterative algorithm [14]. However, these methods have a disadvantage that the optimized product filter may not ensure the existence of a linear phase spectral factor $H(z)$. As a result, the optimized product filter may not lead to the optimal prototype filter. By our formulation (18), the relation between the product filter and its linear phase spectral factor is incorporated in the optimization problem. Unfortunately, the constraint $\mathbf{g} \in \mathcal{C}$ results in nonconvexity of the optimization problem. In the next section, we introduce a relaxation technique to transform the nonconvex problem (18) into an SDP problem.

III. Nonconvexity Analysis and Semidefinite Programming Relaxation

It is observed that the optimization problem (18) is to minimize a (convex) linear objective function subject to the (convex) linear equality constraints and the nonconvex set constraint $\mathbf{g} \in \mathcal{C}$. Therefore, the nonconvexity of the problem (18) mainly depends on the structure of the set $\mathcal{C}$. In this section, we will mathematically analyze the nonconvexity of the set $\mathcal{C}$. In particular, we analyze the rank of nonconvexity, i.e., the number of nonconvex variables, and the degree of nonconvexity, i.e., the extent to which the variables are nonconvex [18].

We introduce the matrix $\mathbf{T}_L(\mathbf{y})$ with $\mathbf{y} = [y_0 \;\; y_1 \ldots y_{2L}]^T$ obtained from $\boldsymbol{\mathcal{T}}_L(\omega)$ by making the change of variables

$$y_i = \cos i\omega, \quad i = 0, 1, \ldots, 2L \tag{19}$$

that is,

$$\mathbf{T}_L(\mathbf{y}) = \begin{bmatrix} y_0 & y_1 & \cdots & y_L \\ y_1 & \frac{y_2+y_0}{2} & \cdots & \frac{y_{L+1}+y_{L-1}}{2} \\ \cdots & \cdots & \ddots & \cdots \\ y_L & \frac{y_{L+1}+y_{L-1}}{2} & \cdots & \frac{y_{2L}+y_0}{2} \end{bmatrix}. \tag{20}$$

Applying the variable change (19) into the set $\mathcal{C}$ in (10) yields

$$\begin{aligned} \mathcal{C} = \{\mathbf{g} \in \mathbb{R}^{N+1} &: \langle \mathbf{g}, \mathbf{y} \rangle \\ &\equiv \langle \mathbf{b}\mathbf{b}^T, \mathbf{T}_L(\mathbf{y}) \rangle \text{ for some } \mathbf{b} \in \mathbb{R}^{L+1}\}. \end{aligned} \tag{21}$$

Equivalently

$$\begin{aligned} \mathcal{C} = \{\mathbf{g} \in \mathbb{R}^{N+1} &: \langle \mathbf{g}, \mathbf{y} \rangle \\ &\equiv \langle \mathbf{X}, \mathbf{T}_L(\mathbf{y}) \rangle, \mathbf{X} \geq 0, \operatorname{rank}(\mathbf{X}) \leq 1\}. \end{aligned} \tag{22}$$

It can be easily verified that the set $\mathcal{C}$ in (22) is not convex due to the rank-one constraint. However, it becomes convex if this constraint is relaxed to rank-two. One of the main results of the paper is the following theorem.

Theorem 1: The polar cone of $\mathcal{C}$ is

$$\mathcal{C}^* = \{\mathbf{y} = [y_0 y_1 \cdots y_{2L}]^T : \mathbf{T}_L(\mathbf{y}) \geq 0\} \tag{23}$$

and convex hull of the nonconvex set $\mathcal{C}$ is defined by

$$\begin{aligned} \operatorname{conv}(\mathcal{C}) &= \{\mathbf{g} \in \mathbb{R}^{N+1} : \langle \mathbf{g}, \boldsymbol{\varphi}_{2L}(\omega) \rangle = \langle \mathbf{h}, \boldsymbol{\varphi}_L(\omega) \rangle^2 \\ &\qquad + \langle \mathbf{q}, \boldsymbol{\varphi}_L(\omega) \rangle^2, \mathbf{h} \in \mathbb{R}^{L+1}, \mathbf{q} \in \mathbb{R}^{L+1}\} \qquad (24) \\ &= \{\mathbf{g} \in \mathbb{R}^{N+1} : \langle \mathbf{g}, \mathbf{y} \rangle = \langle \mathbf{X}, \mathbf{T}_L(\mathbf{y}) \rangle, \\ &\qquad \mathbf{X} \geq 0, \operatorname{rank}(\mathbf{X}) \leq 2)\} \qquad (25) \\ &= \{\mathbf{g} \in \mathbb{R}^{N+1} : \langle \mathbf{g}, \mathbf{y} \rangle = \langle \mathbf{X}, \mathbf{T}_L(\mathbf{y}) \rangle, \mathbf{X} \geq 0\}. \qquad (26) \end{aligned}$$

Proof: The proof is given in the Appendix. ■

The significance of Theorem 1 is that the set $\mathcal{C}$ is nonconvex because of the nonconvex rank-one constraint. However, it becomes convex if the rank-one constraint is replaced by a rank-two constraint. Theorem 1 serves a base for tight convex relaxation for optimization over the nonconvex set $\mathcal{C}$.

Instead of the nonconvex problem (18) we consider the convexified problem

$$\min_{\mathbf{g}} \quad \langle \mathbf{c}, \mathbf{g} \rangle \tag{27a}$$

$$\text{subject to:} \quad g_{2Mi} = \frac{1}{2M}\delta(i), \quad i = 0, 1, \ldots, \left\lfloor \frac{L}{M} \right\rfloor, \tag{27b}$$

$$\mathbf{g} \in \operatorname{conv}(\mathcal{C}) \tag{27c}$$

which is explicitly expressed as an SDP problem

$$\min_{\mathbf{g}, \mathbf{X}} \quad \langle \mathbf{c}, \mathbf{g} \rangle \tag{28a}$$

$$\text{subject to:} \quad g_{2Mi} = \frac{1}{2M}\delta(i), \quad i = 0, 1, \ldots, \left\lfloor \frac{L}{M} \right\rfloor \tag{28b}$$

$$\langle \mathbf{g}, \mathbf{y} \rangle = \langle \mathbf{X}, \mathbf{T}(\mathbf{y}) \rangle, \quad \mathbf{X} \geq 0 \tag{28c}$$

where the matrix variable $\mathbf{X}$ of dimension $(L+1) \times (L+1)$ is equivalent to $(L+1)(L+2)/2$ scalar variables. Deriving g_i from the equality constraints in (28c) and substituting into (28a) and (28b), we obtain[1]

$$\min_{\mathbf{X}} \quad \left\langle \sum_{i=0}^{N} c_i \boldsymbol{\mathcal{M}}_i, \mathbf{X} \right\rangle \tag{29a}$$

$$\text{subject to:} \quad \langle \boldsymbol{\mathcal{M}}_{2Mi}, \mathbf{X} \rangle = \frac{1}{2M}\delta(i), \quad i = 0, 1, \ldots, \left\lfloor \frac{L}{M} \right\rfloor. \tag{29b}$$

$$\mathbf{X} \geq 0. \tag{29c}$$

Note that (29) minimizes a linear function subject to linear equality constraints of a positive semi-definite matrix, therefore it is a standard SDP of equality form. It is well known that the SDP problem can be efficiently solved by modern primal-dual interior-point methods. To find the dual problem associated to the primal problem (28) [or, equivalently, (29)], we use Lagrangian duality. The dual problem of (28) is

$$\max_{\mathbf{y} \in \mathcal{C}^*, \lambda} \min_{\mathbf{g} \in \operatorname{conv}(\mathcal{C})} \left(\langle \mathbf{c}, \mathbf{g} \rangle - \langle \mathbf{y}, \mathbf{g} \rangle + \sum_{i=1}^{\lfloor L/M \rfloor} \lambda_i \left(g_{2Mi} - \frac{\delta(i)}{2M} \right) \right) \tag{30}$$

[1]The authors thank Reviewer 3 for providing the derivation of (29).

where $\mathbf{y} \in \mathcal{C}^*$ is a dual variable and λ_i are Lagrange multipliers associated with equality constraints. It then reduces to

$$\begin{aligned} \max_{\mathbf{y}\in\mathcal{C}^*,\lambda} \quad & \frac{\lambda_0}{2M} \\ \text{subject to:} \quad & c_{2Mi} - y_{2Mi} - \lambda_i = 0, \\ & \qquad\qquad i = 0,1,\ldots,\lfloor L/M \rfloor \\ & c_l - y_l = 0, \quad 1 \le l \ne 2Mi. \end{aligned} \tag{31}$$

Equivalently

$$\begin{aligned} \min_{\mathbf{y}} \quad y_0 : \quad & \mathbf{T}_L(\mathbf{y}) \ge 0, \\ & y_\ell = c_\ell, \quad 1 \le \ell \ne 2Mi,\ i = 1,2,\ldots,\lfloor L/M \rfloor. \end{aligned} \tag{32}$$

The dual optimization problem (32) is also an SDP problem, but its number of scalar variables, $\lfloor L/M \rfloor + 1$, is much less than that of the primal optimization problem (28). The gap between feasible solutions $\mathbf{g}$ and $\mathbf{y}$ of the primal SDP problem (28) and the dual problem (32) is easily derived

$$\langle \mathbf{c}, \mathbf{g} \rangle - \frac{\lambda_0}{2M} = \langle \mathbf{g}, \mathbf{y} \rangle = \langle \mathbf{X}, \mathbf{T}_L(\mathbf{y}) \rangle \tag{33}$$

and then the optimal value $\mathbf{y}_{\text{opt}}$ of the dual problem (32) and $\mathbf{X}_{\text{opt}}$ of the primal problem (28) must satisfy the following complementary condition:

$$\begin{aligned} \langle \mathbf{X}_{\text{opt}}, \mathbf{T}_L(\mathbf{y}_{\text{opt}}) \rangle = 0 \Leftrightarrow \mathbf{b}_k^T \mathbf{T}_L(\mathbf{y}_{\text{opt}}) \mathbf{b}_k \\ = 0 \text{ for } \mathbf{X}_{\text{opt}} = \sum_k \mathbf{b}_k \mathbf{b}_k^T. \end{aligned} \tag{34}$$

The above equation implies that $\mathbf{b}_k$ belong to the null space of matrix $\mathbf{T}_L(\mathbf{y}_{\text{opt}})$. Therefore, if matrix $\mathbf{T}_L(\mathbf{y}_{\text{opt}})$ is of rank L, then matrix $\mathbf{X}_{\text{opt}}$ is rank-one, i.e., $\mathbf{X}_{\text{opt}} = \mathbf{b}_{\text{opt}} \mathbf{b}_{\text{opt}}^T$. It follows that $\mathbf{b}_{\text{opt}}$ is a globally optimal solution of problem (28), and is also a globally optimal solution of problem (18). However, the numerical solution $\mathbf{T}_L(\mathbf{y}_{\text{opt}})$ in general is not guaranteed to be rank L, i.e., matrix $\mathbf{X}_{\text{opt}}$ is not rank one, then an optimal rank-one approximation of $\mathbf{X}_{\text{opt}}$ is given by $\sigma_{\max} \mathbf{u}^{(\max)} \mathbf{u}^{(\max)T}$, where $\mathbf{u}^{(\max)}$ is the eigenvector corresponding to the largest eigenvalue $\sigma_{\max}$ of $\mathbf{X}_{\text{opt}}$. Consequently, the optimal prototype filter is approximated by $\mathbf{b}_{\text{opt}} = \sqrt{\sigma_{(\max)}} \mathbf{u}^{(\max)}$. Our simulation results show that in the most cases the rank of $\mathbf{X}_{\text{opt}}$ is very low so this approximation is highly accurate.

Notice that the feasible region of the original nonconvex problem (18) is a subset of that of the relaxation problem (28), so the stopband energy of the prototype filter obtained form relaxation problem is less than that of the nonconvex problem. However, since the perfect condition is relaxed, the reconstruction error is not well satisfied in some cases. We note, however, that the nonconvex problem has a low rank of nonconvexity, so the solution of the convex relaxation problem is close to being optimal. Therefore, the reconstruction error can be efficiently improved by the following algorithm in next section.

IV. Cheap Iterative Algorithm

The SDP problem (32) is efficiently solved. It can solve large scale problems in which filter order can be of the order of thousands. However, its globally optimal solution results in the globally optimal solution of the nonconvex optimization problem (18) if and only if the optimal positive semi-definite matrix $\mathbf{T}_L(\mathbf{y}_{\text{opt}})$ is of rank L so the optimal matrix $\mathbf{X}_{\text{opt}}$ of (28) is of rank 1. When the filter order is low, the simulation results show that this optimal matrix can be precisely approximated by rank-one matrix, as shown in the following design examples. However, when the filter order is high (about hundreds), the optimal solution is not guaranteed to be rank-one. The reason is that the number of linear constraints imposed on the symmetric matrix $\mathbf{X}$ is $\lfloor (L)/(M) \rfloor + 1$ while the number of scalar variables of matrix $\mathbf{X}$ is $(L+1)(L+2)/2$. Therefore, when the filter order is high, the number of linear constraints increases less than the free parameters. As a result, the approximation of rank-one matrix gives the filter with high stopband attenuation, but the $2M$th band condition is not well satisfied. Then, the simple iterative algorithm can be applied to improve the reconstruction error [3], [20]. Let $\mathbf{b}_0$ denote the optimal prototype filter found by the SDP relaxation problem in Section III, then an iterative algorithm can be given by

$$\begin{aligned} \min_{\mathbf{b}} \quad & \langle \mathbf{b}\mathbf{b}^T, \mathbf{Q} \rangle \\ \text{subject to:} \quad & \langle \mathbf{b}_k \mathbf{b}^T, \boldsymbol{\mathcal{M}}_{2Mi} \rangle = \frac{1}{2M} \delta(i), \quad i = 0,1,\ldots, \left\lfloor \frac{L}{M} \right\rfloor. \end{aligned} \tag{35}$$

By defining

$$\mathbf{A}_k = [\boldsymbol{\mathcal{M}}_0 \mathbf{b}_k \boldsymbol{\mathcal{M}}_{2M} \mathbf{b}_k \cdots \boldsymbol{\mathcal{M}}_{2M\lfloor \frac{L}{M} \rfloor} \mathbf{b}_k]^T \in \mathbb{R}^{(\lfloor \frac{L}{M} \rfloor + 1) \times (L+1)}$$

we can rewrite the optimization problem (35) as

$$\begin{aligned} \min_{\mathbf{b}} \quad & \mathbf{b}^T \mathbf{Q} \mathbf{b} \\ \text{subject to:} \quad & \mathbf{A}_k \mathbf{b} - \frac{1}{2M} \mathbf{e}_1 = 0 \end{aligned} \tag{36}$$

where $\mathbf{e}_1 = [1\ 0\ \cdots\ 0]^T \in \mathbb{R}^{\lfloor \frac{L}{M} \rfloor + 1}$. Then its dual optimization problem is given by

$$\begin{aligned} \min_{\mathbf{b}} \max_{\mathbf{y}} & \left(\mathbf{b}^T \mathbf{Q} \mathbf{b} + \mathbf{y}^T \left(\mathbf{A}_k \mathbf{b} - \frac{1}{2M} \mathbf{e}_1 \right) \right) \\ & = \max_{\mathbf{y}} \min_{\mathbf{b}} \left(\mathbf{b}^T \mathbf{Q} \mathbf{b} + \mathbf{y}^T \left(\mathbf{A}_k \mathbf{b} - \frac{1}{2M} \mathbf{e}_1 \right) \right). \end{aligned} \tag{37}$$

Consequently, it can be shown that its optimal solution $\mathbf{b}_*$ is

$$\mathbf{b}_* = \frac{1}{2M} \mathbf{Q}^{-1} \mathbf{A}_k^T \left(\mathbf{A}_k \mathbf{Q}^{-1} \mathbf{A}_k^T \right)^{-1} \mathbf{e}_1. \tag{38}$$

The iterative algorithm can now be described in terms of the following steps.

Step 1) Chose the prototype filter designed by the method in Section III as the initial filter $\mathbf{b}_0$, and set iteration number $k = 0$.

Step 2) Compute $\mathbf{b}_*$ using (38).

TABLE I
PERFORMANCE COMPARISON OF THE DESIGN IN EXAMPLE 1

	Prototype filter			E_{pp}	E_a
	N	ω_s	A_s (dB)		
Method of [19]	39	0.120π	35	$10.810 \cdot 10^{-3}$	$2.259 \cdot 10^{-3}$
Proposed method	40	0.120π	35.8	$5.508 \cdot 10^{-3}$	$2.477 \cdot 10^{-3}$

Step 3) Update $\mathbf{b}_{k+1} = \tau\mathbf{b}_k + (1-\tau)\mathbf{b}_*$, where the weight $\tau \in (0,1)$. Then, normalize the DC gain by $\mathbf{b}_{k+1} \longleftarrow (\mathbf{b}_{k+1}/\mathbf{1}^T\mathbf{b}_{k+1})$, where vector $\mathbf{1} = [1,1,\ldots,1]^T$.

Step 4) If $\max_{i=0,1,\ldots,\lfloor L/M \rfloor} |\mathbf{b}_{k+1}^T \boldsymbol{\mathcal{M}}_{2Mi} \mathbf{b}_{k+1} - \delta(i)/2M| \leq \epsilon$, where ϵ is a prescribed tolerance, then the iteration algorithm is terminated, and $\mathbf{b}_{\text{opt}} = \mathbf{b}_{k+1}$. Otherwise set $k = k+1$ and go to Step 2).

It is noted that the proposed iterative algorithm is very computationally efficient since the closed-form solution is obtained in each iteration. Moreover, the $(L+1)\times(L+1)$ matrix $\mathbf{Q}$ does not change in the iteration, so $\mathbf{Q}^{-1}$ is computed only once outside the iteration. In addition, the optimal solution of convex relaxation is used as the initial point for the iterative algorithm, and as a result the proposed algorithm converges very fast to an optimal solution. Simulation results show that the algorithm converges in fewer than ten iterations.

V. DESIGN EXAMPLES

In this section, we provide several examples to illustrate the performance of the methods described in the previous sections. Discussion on their effectiveness is also given. The performance of the filter banks is evaluated in the terms of the stopband attenuation of filters, reconstruction error, and aliasing error. The performance criteria are as follows:

- stopband attenuation $A_s = -20\log_{10}\delta_s$, where $\delta_s = \max_{\omega\in[\omega_s\,\pi]}|H(e^{j\omega})|$;
- the maximum peak to peak reconstruction error

$$E_{\text{pp}} = \max_{\omega}(MT_0(e^{j\omega})) - \min_{\omega}(MT_0(e^{j\omega}));$$

- the peak aliasing distortion

$$E_a = \max_{\omega} E(e^{j\omega})$$

where

$$E(e^{j\omega}) = \left[\sum_{l=1}^{M-1} |T_l(e^{j\omega})|^2\right]^{1/2}.$$

It should be noted that for cosine-modulated pseudo-QMF banks the high stopband attenuation results in the small aliasing error. However, high stopband attenuation characteristic and small reconstruction error ripples are conflicting objectives. The following examples will show the performance tradeoff of the proposed methods.

A. Designs Using the SDP Relaxation Method

The SDP relaxation problem presented in Section III is used to design cosine-modulated QMF banks in this subsection. All SDP optimization problems presented here are solved using an available SDP solver, SeDuMi [15]. All designs are carried out by using Matlab version 6.5 on a Pentium IV 3-GHz PC.

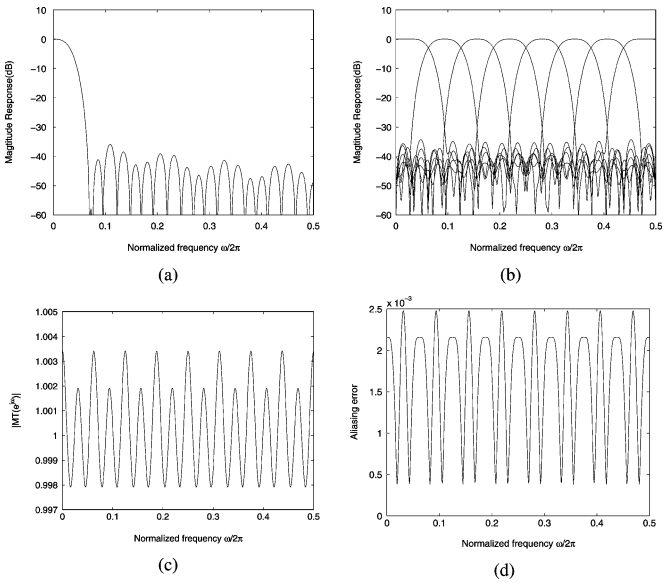

Fig. 2. Example 1. (a) Magnitude response of the optimized prototype $H(e^{j\omega})$; (b) magnitude responses of the analysis filters $H_k(e^{j\omega})$; (c) magnitude response plot for the overall distortion $M|T(e^{j\omega})|$; (d) magnitude response plot for the aliasing error $E(e^{j\omega})$.

Example 1: An eight-channel cosine-modulated pseudo-QMF bank is designed. The prototype filter has the specifications: $N = 40, K = 1, W_1 = 1, \omega_0 = \omega_s = 0.120\pi$ and $\omega_1 = \pi$. It took SeDuMi solver about 0.49 s to find the optimal prototype filter. The magnitude responses of the optimized prototype filter $H(e^{j\omega})$, the corresponding analysis filters $H_k(e^{j\omega})$, the overall distortion function $M|T_0(e^{j\omega})|$, and the aliasing error function $E(e^{j\omega})$ are plotted in Fig. 2, respectively. Note that the stopband attenuation of $H(e^{j\omega})$ and $H_k(e^{j\omega})$ is about 35.8 dB, the maximum peak-to-peak reconstruction error is $E_{pp} = 5.508 \cdot 10^{-3}$, and the maximum of the aliasing error is $E_a = 2.477 \cdot 10^{-3}$. The comparison of our result with that of the nonlinear optimization based method in [19] is shown in Table I. It can seen that our proposed method can significantly improve the reconstruction error.

Example 2: In this example, a 17-channel cosine modulated pseudo-QMF bank, which the prototype filter has the specifications: $N = 102, K = 1, W_1 = 1, \omega_0 = \omega_s = 0.0590\pi$ and $\omega_1 = \pi$, is designed. It took SeDuMi solver about 2.16 s to find the optimal prototype filter. Fig. 3(a) and (b) shows the magnitude responses of the optimized prototype filter $H(e^{j\omega})$ and, the corresponding analysis filters $H_k(e^{j\omega})$, respectively. Fig. 3(c) and (d), respectively, shows the magnitude responses of the overall distortion function $M|T_0(e^{j\omega})|$, and the aliasing

TABLE II
PERFORMANCE COMPARISON OF THE DESIGN IN EXAMPLE 2

	Prototype filter				
	N	ω_s	A_s (dB)	E_{pp}	E_a
Method of [19]	101	0.0590π	40.65	$6.790 \cdot 10^{-3}$	$3.794 \cdot 10^{-4}$
Proposed method	102	0.0590π	45	$5.9566 \cdot 10^{-3}$	$3.8948 \cdot 10^{-4}$

TABLE III
PERFORMANCE COMPARISON DESIGN IN EXAMPLE 3

	Prototype filter					No. of iterations	CPU time second per iteration
	N	ω_s	A_s (dB)	E_{pp}	E_a		
Method of [10]	466	0.03207π	100	$39.749 \cdot 10^{-4}$	$3.8618 \cdot 10^{-7}$	N/A	N/A
Method of [11]	447	0.03125π	100	$21.8 \cdot 10^{-4}$	$1.9900 \cdot 10^{-7}$	287	0.7104
Proposed method	466	0.03125π	102	$9.121 \cdot 10^{-4}$	$2.3818 \cdot 10^{-7}$	3	0.0107

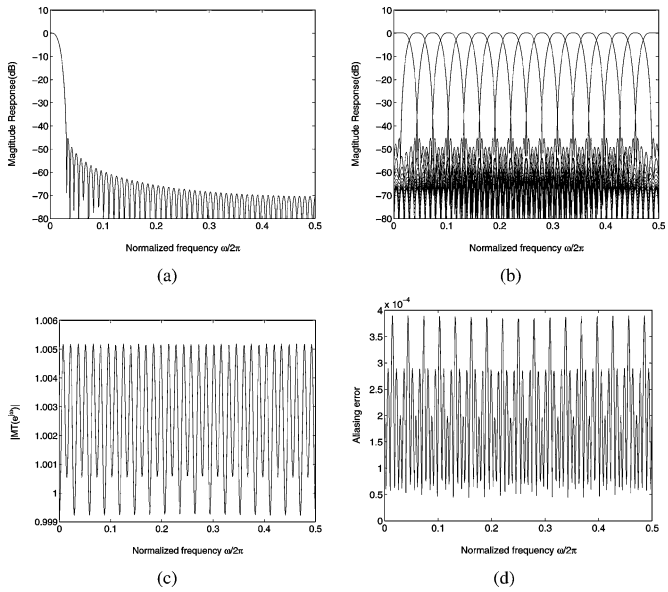

Fig. 3. Example 2. (a) magnitude response of the optimized prototype $H(e^{j\omega})$; (b) magnitude responses of the analysis filters $H_k(e^{j\omega})$; (c) magnitude response plot for the overall distortion $M|T(e^{j\omega})|$; (d) magnitude response plot for aliasing error $E(e^{j\omega})$.

error function $E(e^{j\omega})$. Table II provides a performance comparison between the proposed method and the method in [19]. In this design, our resulting filter has much higher stopband attenuation than the resulting filter in [19] while other performances are almost identical.

Remarks: The simulation results show that the SDP relaxation can provide the filter banks with higher performance as compared to nonlinear nonconvex optimization methods for low-order filters. Moreover, it is also noted that the proposed method is based on SDP, so the optimal solution is efficiently found without depending on any initial points. Conversely, the resulting filter in [19] is found from highly nonlinear nonconvex optimization, so its solution is very sensitive to initialization.

B. Designs Using the Cheap Iterative Algorithm

As mentioned earlier, in the cases where the filter order is high, the approximation of matrix rank-one is not precise. As a result, the resulting filter has still high stopband attenuation, but the reconstruction error needs to be further improved. In following designs, the cheap iterative algorithm in Section IV is applied with an initial point b_0 obtained from the SDP relaxation method.

Example 3: This example considers the design of a 32-channel cosine-modulated filter bank. The specifications for the design of the prototype filter are $N = 466, K = 3, W_1 = 3, W_2 = 1.2, W_3 = 1, \omega_0 = \omega_s = 0.03125\pi, \omega_1 = 0.050625\pi, \omega_2 = 0.225\pi$ and $\omega_3 = \pi$. It took SeDuMi solver about 32.70 s to design the initial filter. With $\epsilon = 6 \cdot 10^{-6}$, the algorithm converges to the optimal filter only in four iterations with an average CPU time of 0.0107 s per iteration. The performance of the resulting filter bank is shown in Fig. 4. It is observed that the stopband attenuation is about 102 dB, the peak-to-peak reconstruction error is $8.985 \cdot 10^{-4}$, and the maximum aliasing error is $1.9686 \cdot 10^{-7}$. Table III provides a performance comparison between the proposed method and the methods in [10], [11]. It can be seen that our proposed method offers much better performance than the method in [10]. As compared to the method [11], our performance can be comparable, but our algorithm is significantly faster.

Example 4: In order to illustrate the tradeoff between the stopband attenuation and the reconstruction error, we consider the design of a 32-channel cosine-modulated filter bank with specifications: $N = 512, K = 1, W_1 = 1, \omega_0 = \omega_s = 0.0315\pi$, and $\omega_1 = \pi$. It took SeDuMi solver about 49.98 s to find the initial filter. First, we choose the tolerance $\epsilon = 3 \cdot 10^{-5}$. The algorithm converges to the optimal filter only in two iterations with an average CPU time of 0.0315 s per iteration. The magnitude responses of the optimized prototype filter $H(e^{j\omega})$, the corresponding analysis filters $H_k(e^{j\omega})$, the overall distortion function $M|T_0(e^{j\omega})|$, and the aliasing error function $E(e^{j\omega})$ are depicted in Fig. 5. It can be seen that the stopband attenuation of $H(e^{j\omega})$ and $H_k(e^{j\omega})$ is about 114 dB, the maximum peak-to-peak reconstruction error is $E_{\rm pp} = 3.0832 \cdot 10^{-3}$, and the maximum of the aliasing error is $E_a = 3.3043 \cdot 10^{-8}$. This performance is comparable to that of Example 1 in [4]. However, our proposed method here is significantly faster since the closed-form expression is obtained in iteration procedure. In another design, we further restrict the $2M$th band constraint by choosing the tolerance $\epsilon = 10^{-7}$, then the algorithm converges in five iterations. The design performance is shown in Fig. 6.

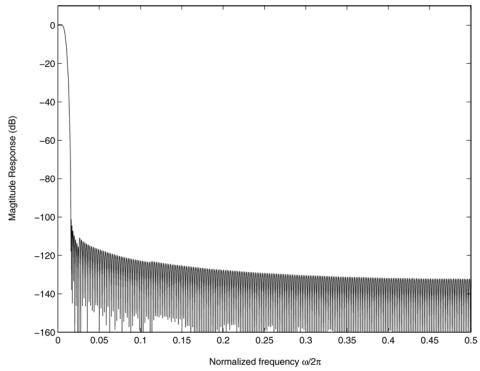

(a)

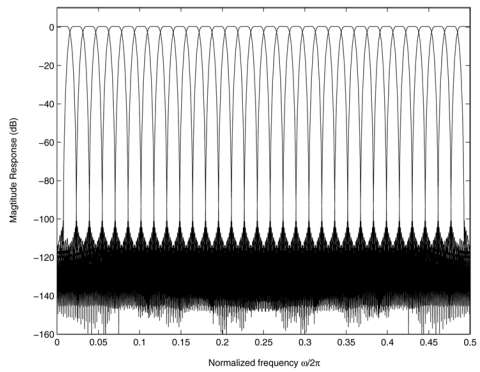

(b)

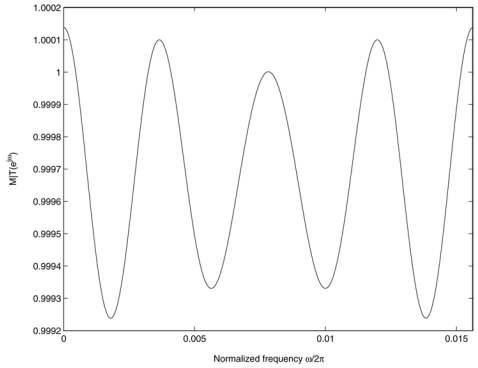

(c)

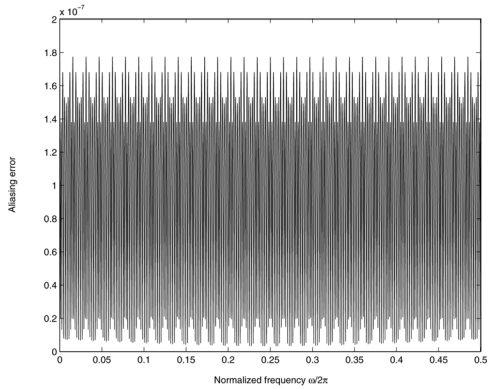

(d)

Fig. 4. Example 3. (a) magnitude response of the optimized prototype $H(e^{j\omega})$; (b) magnitude responses of the analysis filters $H_k(e^{j\omega})$; (c) magnitude response plot for the overall distortion $M|T(e^{j\omega})|$ on $[0, \pi/M]$; (d) magnitude response plot of the aliasing error $E(e^{j\omega})$.

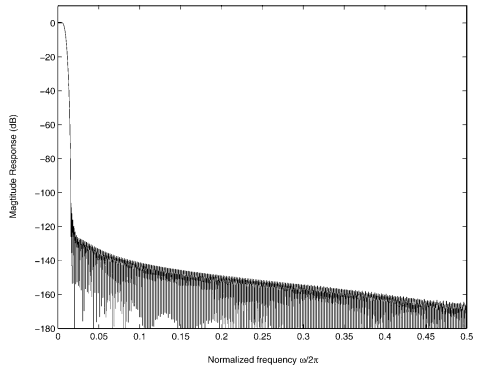

(a)

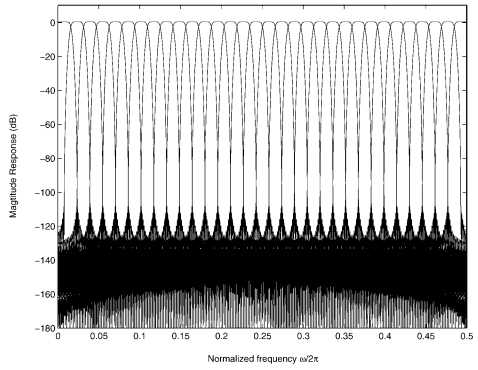

(b)

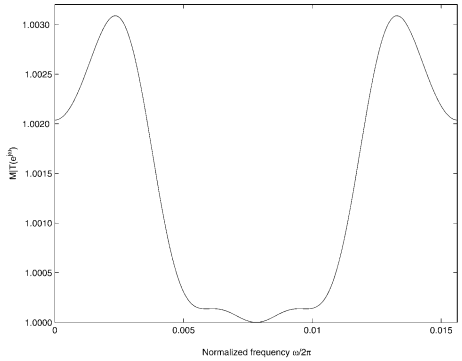

(c)

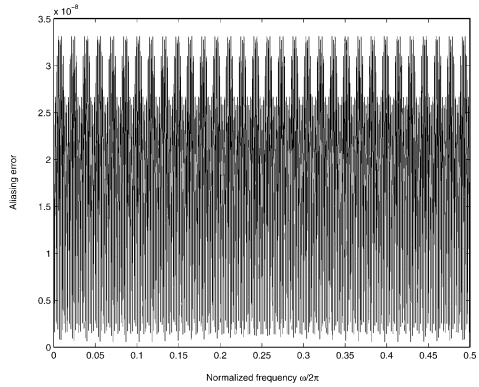

(d)

Fig. 5. Example 4. (a) magnitude response of the optimized prototype $H(e^{j\omega})$; (b) magnitude response plots for the analysis filters $H_k(e^{j\omega})$; (c) magnitude response plot for the overall distortion $M|T(e^{j\omega})|$ on $[0, \pi/M]$; (d) magnitude response plot of aliasing error $E(e^{j\omega})$.

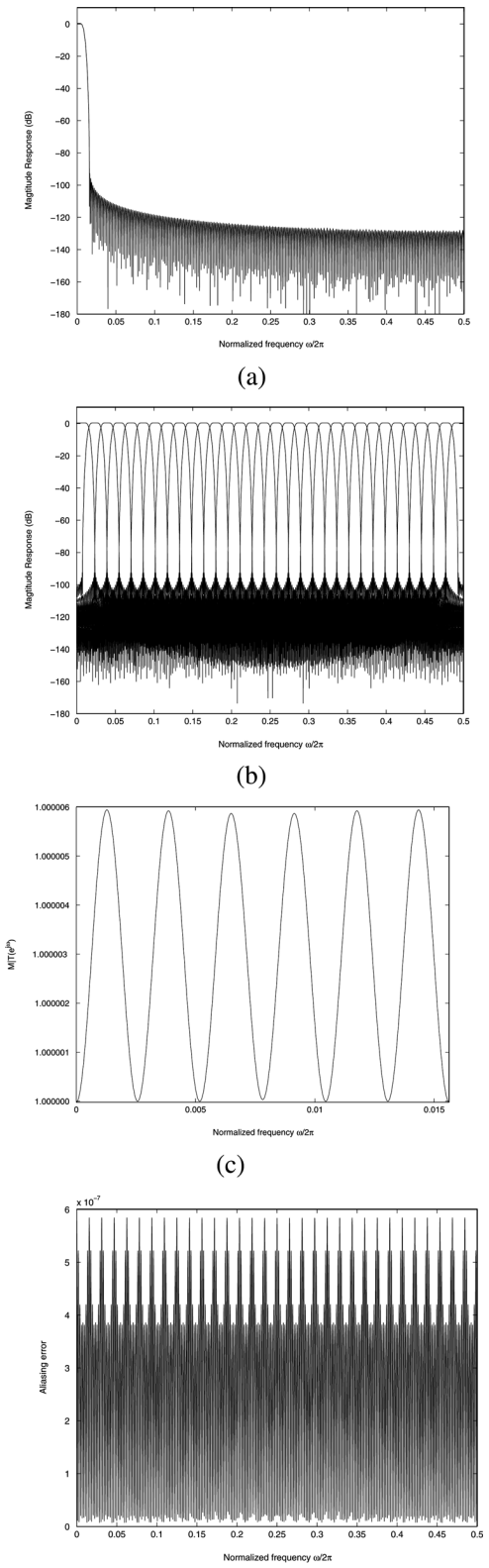

Fig. 6. Example 4. (a) magnitude response of the optimized prototype $H(e^{j\omega})$; (b) magnitude response plots for the analysis filters $H_k(e^{j\omega})$; (c) magnitude response plot for the overall distortion $M|T(e^{j\omega})|$ on $[0, \pi/M]$; (d) magnitude response plot of aliasing error $E(e^{j\omega})$.

We can see that the stopband attenuation of the prototype filter is now about 96 dB, the maximum peak to peak reconstruction error is $E_{\rm pp} = 5.9582 \cdot 10^{-6}$, and the maximum of the aliasing error is $E_a = 5.8315 \cdot 10^{-7}$. This design offers better stopband attenuation than the design using method in [3]. On the other hand, these two designs illustrate that the reconstruction error can be improved at the expense of the stopband attenuation reduction.

VI. Concluding Remarks

Efficient designs for optimizing the prototype filter of CMFBs have been presented. First, we have shown that the CMFB design problem can be cast into a convex SDP problem by using the convex relaxation technique. Compared to the nonconvex nonlinear optimization based designs in [19], which the resulting prototype filter is sensitive to the initial filter, our method can be effectively solved by SDP techniques. Moreover, the linear phase optimal prototype filter can be efficiently obtained by the singular value decomposition of the optimal matrix instead of the conventional spectral factorization. For filters with large order, the reconstruction error can be further improved by the cheap iterative algorithm in which the closed-form expression is provided in each iteration.

Appendix
The Proof of Theorem 1

For the proof, we need the following result

Lemma 1: Define

$$\boldsymbol{\psi}_L(t) = [1 \ t \cdots t^L]^T.$$

Any $2L$th-order nonnegative real polynomial is not necessarily a square but always a sum of two squares:

$$P(t) \geq 0 \Leftrightarrow P(t) = \langle \mathbf{x}, \boldsymbol{\psi}_L(t)\rangle^2 + \langle \mathbf{y}, \boldsymbol{\psi}_L(t)\rangle^2, \ \mathbf{x} \in \mathbb{R}^{L+1}, \quad \mathbf{y} \in \mathbb{R}^{L+1} \tag{39}$$

$$\Leftrightarrow P(t) = \langle \mathbf{x}\mathbf{x}^T + \mathbf{y}\mathbf{y}^T, \mathbf{M}_L(t)\rangle, \mathbf{M}_L(t) = \boldsymbol{\psi}_L(t)\boldsymbol{\psi}_L^T(t). \tag{40}$$

Proof of Lemma 1[2]:As $P(t) \geq 0 \ \forall t \in \mathbb{R}$, every its real root must have even multiplicity, so the factor of $P(t)$ corresponding to the real roots is a square. On the other hand the factors corresponding to complex roots of conjugate pairs are sums of two squares because for any root $z = a + jb$

$$(t - z)(t - \bar{z}) = (t - a)^2 + b^2.$$

Now, $P(t)$ is a sum of two squares because if $h_i(t) = p_i^2(t) + q_i^2(t), \mathrm{i} = 1, 2$, then their product is still a sum of two squares:

$$h_1(t)h_2(t) = (p_1(t)p_2(t) + q_1(t)q_2(t))^2 + (q_1(t)p_2(t) - p_1(t)q_2(t))^2.$$

□

[2]This short proof is by Dr. Hung Q. Ngo.

Proof of Theorem 1: Using the definition (21) of the set $\mathcal{C}$, one has

$$\begin{aligned}\mathbf{y} \in \mathcal{C}^* &\Leftrightarrow \langle \mathbf{y}, \mathbf{g} \rangle \geq 0, \forall \mathbf{g} \in \mathcal{C} \\ &\Leftrightarrow \langle \mathbf{b}\mathbf{b}^T, \mathbf{T}_L(\mathbf{y}) \rangle \geq 0, \forall \mathbf{b} \in \mathbb{R}^{L+1} \\ &\Leftrightarrow \mathbf{T}_L(\mathbf{y}) \rangle \geq 0\end{aligned}$$

showing (23).

Next, suppose $\mathrm{conv}_1(\mathcal{C})$ and $\mathrm{conv}_2(\mathcal{C})$ are the set defined by the right-hand side of (24)/(25) and (26), respectively.
Notice that any $\mathbf{X} \geq 0$ admits the SVD $\mathbf{X} = \sum_k \mathbf{b}_k \mathbf{b}_k^T$, so

$$\langle \mathbf{X}, \mathbf{T}_L(\mathbf{y}) \rangle = \sum_k \left\langle \mathbf{b}_k \mathbf{b}_k^T, \mathbf{T}_L(\mathbf{y}) \right\rangle$$

implying that $\mathrm{conv}_2(\mathcal{C}) \subset \mathrm{conv}(\mathcal{C})$. This together with the relation $\mathrm{conv}(C) \subset \mathrm{conv}_2(\mathcal{C})$ by the definition of $\mathrm{conv}(\mathcal{C})$ gives $\mathrm{conv}_2(\mathcal{C}) = \mathrm{conv}(\mathcal{C})$.
To complete the proof of the Theorem, it remains to show $\mathrm{conv}_1(\mathcal{C}) = \mathrm{conv}_2(\mathcal{C})$. As it is obvious that $\mathrm{conv}_1(\mathcal{C}) \subset \mathrm{conv}_2(\mathcal{C})$ it is sufficient to show the inverse inclusion $\mathrm{conv}_2(\mathcal{C}) \subset \mathrm{conv}_1(\mathcal{C})$.

Let A_L be the nonsingular matrix such that $\boldsymbol{\psi}_L(\cos\omega) = \mathbf{A}_L \boldsymbol{\varphi}_L(\omega)$ (for the existence of $\mathbf{A}_L$ see [16]). Let $\mathbf{g} \in \mathrm{conv}_2(\mathcal{C})$. From the definition (26), there are $\mathbf{b}_k \in \mathbb{R}^{L+1}$ such that

$$\begin{aligned}\langle \mathbf{g}, \boldsymbol{\varphi}_{2L}(\omega) \rangle &= \sum_k \langle \mathbf{b}_k, \boldsymbol{\varphi}_L(\omega) \rangle^2 \\ &= \langle \mathbf{g}, \boldsymbol{\varphi}_{2L}(\omega) \rangle = \sum_k \langle \bar{\mathbf{b}}_k, \boldsymbol{\psi}_L(\cos\omega) \rangle^2 \\ \bar{\mathbf{b}}_k &= \mathbf{A}_L^{-T} \mathbf{b}_k.\end{aligned}$$

For $\bar{\mathbf{b}}_k$, by Lemma 1 there are $\tilde{\mathbf{b}}_1$ and $\tilde{\mathbf{b}}_2$ such that

$$\sum_k \langle \bar{\mathbf{b}}_k, \boldsymbol{\psi}_L(\cos\omega) \rangle^2 = \sum_{i=1}^{2} \langle \tilde{\mathbf{b}}_i, \boldsymbol{\psi}_L(\cos\omega) \rangle^2$$

so

$$\langle \mathbf{g}, \boldsymbol{\varphi}_{2L}(\omega) \rangle = \sum_{i=1}^{2} \langle \mathbf{x}_k, \boldsymbol{\varphi}_L(\omega) \rangle^2, \quad \mathbf{x}_k = \mathbf{A}_L^T \tilde{\mathbf{b}}_k$$

showing that $\mathbf{g} \in \mathrm{conv}_1(\mathcal{C})$. The proof of the Theorem is complete.

ACKNOWLEDGMENT

The authors would like to thank the anonymous reviewers and the associate editor for their valuable comments which helped to greatly improve the quality of the paper.

REFERENCES

[1] A. N. Akansu and R. A. Haddad, *Multiresolution Signal Decomposition: Transforms, Subbands, Wavelets*. New York: Academic, 2001.

[2] C. D. Creusere and S. K. Mitra, "A simple method for designing high quality prototype filters for M-band pseudo-QMF banks," *IEEE Trans. Signal Process.*, vol. 43, no. 4, pp. 1005–1007, Apr. 1995.

[3] Y.-T. Fong and C.-W. Kok, "Iterative least squares design of DC-leakage free paraunitary cosine modulated filter banks," *IEEE Trans. Circuits Syst. II, Analog Digit. Signal Process.*, vol. 50, no. 5, pp. 238–243, May 2003.

[4] M. B. Furtado, P. S. R. Diniz, and S. L. Netto, "Numerically efficient optimal design of cosine-modulated filter banks with peak-constrainted least-squares behavior," *IEEE Trans. Signal Process.*, vol. 52, no. 3, pp. 597–608, Mar. 2005.

[5] P. N. Heller, T. Karp, and T. Q. Nguyen, "A general formulation of modulated filter banks," *IEEE Trans. Signal Process.*, vol. 47, no. 4, pp. 986–1002, Apr. 1999.

[6] O. G. Ibarra-Manzano and G. Jovanic-Dolecek, "Cosine-modulated FIR filter banks satisfying perfect reconstruction: An iterative algorithm," in *Proc. 42nd Midwest Symp. Circuits Systems*, Aug. 1999, vol. 2, pp. 1061–1064.

[7] H. H. Kha, H. D. Tuan, and T. Q. Nguyen, "Design of cosine-modulated pseudo-QMF banks using semidefinite programming relaxation," in *Proc. IEEE Int. Symp. Circuits Systems (ISCAS)*, New Orleans, LA, May 2007.

[8] H. H. Kha, H. D. Tuan, and T. Q. Nguyen, "An efficient SDP based design for prototype filters of M-channel cosine-modulated filter banks," in *Proc. IEEE Int. Conf. Acoustics, Speech Signal Processing (ICASSP)*, May 2007, vol. 3, pp. III-893–III-896.

[9] R. D. Koilpillai and P. P. Vaidyanathan, "A spectral factorization approach to pseudo-QMF design," *IEEE Trans. Signal Process.*, vol. 41, no. 1, pp. 82–92, Jan. 1993.

[10] Y. P. Lin and P. P. Vaidyanathan, "A Kaiser window approach for the design of prototype filters of cosine modulated filterbanks," *IEEE Signal Process. Lett.*, vol. 5, no. 6, pp. 132–134, Jun. 1998.

[11] W.-S. Lu, T. Saramaki, and R. Bregovic, "Design of practically perfect-reconstruction cosine-modulated filter banks: A second-order cone programming approach," *IEEE Trans. Circuits Syst.*, vol. 51, no. 3, pp. 552–563, Mar. 2004.

[12] T. Q. Nguyen, "Near-perfect-reconstruction pseudo-QMF banks," *IEEE Trans. Signal Process.*, vol. 42, no. 1, pp. 65–76, Jan. 1994.

[13] T. Q. Nguyen, "Digital filter bank design quadratic-constrained formulation," *IEEE Trans. Signal Process.*, vol. 43, no. 9, pp. 2103–2108, Sep. 1995.

[14] G. Strang and T. Q. Nguyen, *Wavelets and Filter Banks*. Wellesley, MA: Wellesley-Cambridge, 1997.

[15] J. F. Sturm, "Using SeDuMi 1.02, a Matlab toolbox for optimization over symmetric cones," *Optimiz. Methods Softw.*, vol. 11–12, pp. 625–653, 1999.

[16] H. D. Tuan, T. T. Son, B. Vo, and T. Q. Nguyen, "Efficient large-scale filter/filterbank design via LMI characterization of trigonometric curves," *IEEE Trans. Signal Process.*, vol. 55, no. 9, pp. 4393–4404, Sep. 2007.

[17] J. Tuqan and P. P. Vaidyanathan, "A state space approach to the design of globally optimal FIR energy compaction filters," *IEEE Trans. Signal Process.*, vol. 48, no. 10, pp. 2822–2838, Oct. 2000.

[18] H. Tuy, *Convex Analysis and Global Optimization*. Norwell, MA: Kluwer, 1997.

[19] P. Vaidyanathan, *Multirate Systems and Filter Banks*. Englewood Cliffs, NJ: Prentice-Hall, 1993.

[20] Z. Zhang, "Design of cosine modulated filter banks using iterative Lagrange multiplier method," in *Proc. IEEE Int. Symp. Mircowave, Antenna, Propagation EMC Technologies for Wireless Communications*, 2005, vol. 1, pp. 157–160.

Ha Hoang Kha received the B.E. and M.E. degrees in electrical engineering and telecommunications from HoChiMinh City University of Technology, in 2000 and 2003, respectively. He has been working towards the Ph.D. degree at the School of Electrical Engineering and Telecommunications, University of New South Wales, Sydney, Australia, since 2004.

His research interests are in digital signal processing, filter banks and wavelets, and their applications in image processing and digital communications.

Hoang Duong Tuan was born in Hanoi, Vietnam, in 1964. He received the Diploma and Ph.D. degrees, both in applied mathematics, from Odessa State University, Ukraine, in 1987 and 1991, respectively.

From 1991 to 1994, he was a Researcher at Optimization and Systems division, Vietnam National Center for Science and Technologies. He spent nine academic years in Japan as an Assistant Professor at the Department of Electronic-Mechanical Engineering, Nagoya University, from 1994 to 1999 and then as an Associate Professor at the Department of Electrical and Computer Engineering, Toyota Technological Institute, Nagoya, from 1999 to 2003. Presently, he is living in Sydney, Australia, where he is an Associate Professor at the School of Electrical Engineering and Telecommunications, University of New South Wales, Sydney, Australia. His research interests include theoretical developments and applications of optimization based methods in many areas of control, signal processing, communication, and bio-informatics.

Truong Q. Nguyen received the B.S., M.S., and Ph.D. degrees in electrical engineering from the California Institute of Technology, Pasadena, in 1985, 1986, and 1989, respectively.

He was a Member of Technical Staff with MIT Lincoln Laboratory from June 1989 to July 1994. From August 1994 to July 1998, he was with the Electrical and Computer Engineering Department, University of Wisconsin, Madison. He was with Boston University from 1996 to 2001, and he is currently with the Electrical and Computer Engineering Department at the University of California in San Diego. His research interests are in the theory of wavelets and filter banks and applications in image and video compression, telecommunications, bioinformatics, medical imaging and enhancement, and analog–digital conversion. He is the coauthor (with Prof. G. Strang) of a popular textbook *Wavelets & Filter Banks* (Wellesley-Cambridge Press, 1997) and the author of several Matlab-based toolboxes on image compression, electrocardiogram compression, and filter bank design. He also holds a patent on an efficient design method for wavelets and filter banks and several patents on wavelet applications including compression and signal analysis.

Prof. Nguyen received the IEEE TRANSACTIONS IN SIGNAL PROCESSING Paper Award (Image and Multidimensional Processing area) for the paper he coauthored with Prof. P. P. Vaidyanathan on linear-phase perfect-reconstruction filter banks (1992). He received the NSF Career Award in 1995 and is currently the Series Editor (Digital Signal Processing) for Academic Press. He served as Associate Editor for the IEEE TRANSACTIONS ON SIGNAL PROCESSING from 1994 to 1996 and for the IEEE TRANSACTION ON CIRCUITS AND SYSTEMS from 1996 to 1997.